Machine-learning-based prediction of a scalar source location from remote sensors in turbulent channel flow

Changbeom Kim
Department of Mechanical Engineering
Seoul National University
Seoul 08826, Republic of Korea
knight627@snu.ac.kr

Sehyeong Oh
Air Science Research Center
Samsung Advanced Institute of Technology
Suwon-si, Gyeonggi-do 16678, Republic of Korea
sehyeong.oh@samsung.com

Haecheon Choi
Department of Mechanical Engineering
Seoul National University
Seoul 08826, Republic of Korea
choi@snu.ac.kr

ABSTRACT

We employ a machine learning approach to identify the location of a scalar source in turbulent channel flow using remote sensor measurements. A source is positioned inside the channel, while sensors are located at downstream locations. For a given source location, the resulting passive scalar signals are recorded at the sensor locations. By systematically varying the source location, a dataset comprising sensor signals and corresponding source locations and strengths is generated. This dataset is used to train a Residual Network (ResNet), by minimizing the root-mean-square error between the predicted and actual source coordinates and strengths. The distance errors predicted by ResNet range from 0.12h to 0.40h (where h is the channel half-height) which is small compared to the size of the whole domain. The smallest errors are observed when the source is located near the channel center, while the largest errors occur when the source is located near the wall. The prediction time is very fast, making the method suitable for real-time applications.

INTRODUCTION

As the semiconductor industry continues to miniaturize, semiconductor device sizes keep shrinking. Consequently, even very small gaseous pollutants (sources) released in semiconductor fabs can affect product quality and yield. Therefore, it is important to predict the locations of such unexpected sources quickly and accurately.

Various methods, including probabilistic inference, optimization, and deep learning classification, have been suggested for source prediction in turbulent flows. However, all of them involve trade-offs between accuracy and computational speed. Among these approaches, the adjoint variational method by Wang *et al*. (2019) has strong mathematical formulation and accuracy. It finds source positions by solving adjoint partial differential equations using both the entire flow field and sensor data. However, its implementation requires whole flow field information and considerable computation time. Thus, this approach is not suitable for practical use in semiconductor fabs, where fast and real-time source detection is required.

In the present study, we suggest a machine-learning-based prediction method that finds source locations quickly and accurately using sensor data only, without knowing flow field data.

METHODS

Numerical details

To obtain the data for training, we perform direct numerical simulation (DNS) to solve turbulent channel flow at a friction Reynolds number ($Re_\tau = u_\tau h/\nu$) of 180, where u_τ is the wall-shear velocity, h is the channel half-height, and ν is the kinematic viscosity. The computational domain size is $Lx \times Ly \times Lz = 2\pi h \times \pi h \times 0.5\pi h$ with approximately 1.2 million grid points. Spatial derivatives are discretized using second-order central differences. For time advancement, third-order Runge-Kutta method and second-order Crank-Nicolson method are used for convection and diffusion terms, respectively.

Given a source location, we solve the continuity, Navier-Stokes, and passive scalar equations to obtain the time-series passive scalar signals at the sensor locations. The source is assumed to be a passive scalar. All sources are generated on the mid-spanwise plane, z/h=π/4. Passive scalar transport equation with source term $\phi(\mathbf{x})$ is

$$\left(\frac{\partial}{\partial t} + u_j \frac{\partial}{\partial x_j} - \frac{1}{ReSc} \frac{\partial^2}{\partial x_j \partial x_j} \right) c = \phi(\mathbf{x}), \tag{1}$$

where c is a passive scalar, Sc is the Schmidt number, and $\phi(\mathbf{x})$ is modeled as (Wang *et al*. 2019)

$$\phi(\mathbf{x}) = \frac{3}{8(\pi - 6/\pi)R^3} \left[\cos\left(\frac{\|\mathbf{x} - \mathbf{x}_s\|}{R} \pi \right) + 1 \right] \left[\mathrm{sign}\left(1 - \frac{\|\mathbf{x} - \mathbf{x}_s\|}{R} \right) + 1 \right] \tag{2}$$

where $\mathbf{x}_s$ is the source center, and R is the spherical radius. The Schmidt number for ammonia is Sc = 0.7 (Massman 1998; Gualtieri et al. 2017) to reflect the fab environment. For spatial discretization, second-order central difference method is applied in y and z directions and a third-order QUICK scheme is applied to the convection term in x direction. For time advancement, second-order Adams-Bashforth and second-order Crank-Nicolson methods are used for convection and diffusion terms, respectively.

Sensor arrangement and dataset construction

Figure 1 shows the source and sensor arrangement. All sensors are located at $x/h = 5.52$: sensors are located at 67 different y locations and 22 different z locations, giving a total of 1474 sensor locations. The time-series data measured by these sensors are converted into a three-dimensional input tensor whose size is 67 × 22 × 1000, where the first two numbers represent the sensor locations, and the third is number of different time instants. The time period recorded is $Tu_\tau/h = 0.85$.

For each source location (x_s, y_s) at $z/h = \pi/4$, the governing equations are solved from a turbulent channel flow at a source release time t_o. Although three different source strengths are considered, only one simulation per source location is required owing to the linear nature of the passive scalar equation. Total 108 different source locations are selected and resulting signals measured by sensors are recorded. The same procedure is repeated for 30 different source-release times. As a result, a total of 9,720 datasets are obtained. Each dataset consists of the 3D sensor data as input and the corresponding source location and strength as output.

Neural network model

These datasets are used to train a 3D ResNet-50 where 50 denotes the number of layers, that maps sensor signals directly to the source location and strength (Fig. 2). This neural network consists of two stem convolutions, four identity residual blocks, 1 × 2 × 2 max-pooling for spatial downsampling, and global average pooling followed by two fully connected layers. While the original ResNet is designed for classification, the final fully connected layers are modified to perform regression so that the network predicts source location and strength. The ResNet is optimized to minimize the root-mean-square error between the predicted and actual source location and strength. This architecture allows the model to exploit both the spatial arrangement of the sensors and the temporal variation of the scalar signals.

RESULTS

The prediction model is tested using data that are not used during training. The test dataset contains 20 source locations, consisting of four streamwise positions and five wall-normal positions from the channel center to the near-wall region (Fig. 1). All test signals are obtained at source-release times that are entirely different from those used for training data.

The prediction distance error is defined as the distance between the predicted and actual source locations. As shown in Fig. 3, the averaged prediction error ranges from $0.12h$ to $0.40h$. The smallest errors are observed when the source is located near the channel center, while the largest errors occur when the source is located near the wall.

When the source is located at the channel center, the predicted locations are tightly clustered around the actual source position. In contrast, when the source is located near the wall, the predictions are widely scattered. This indicates that near-wall sources are more difficult to identify from downstream sensor signals. However, even in the near-wall cases, the predictions remain largely confined to the near-wall region. This shows that the wall-normal location of the source is still well captured, while its streamwise position exhibits larger uncertainty.

This result can be explained from the flow physics. Near the wall, strong shear enhances the deformation and spreading of the scalar plume. As a result, the scalar field becomes more diffused and its magnitude is quickly reduced, making it harder for the model to identify the upstream source location. Furthermore, for near-wall sources, the scalar signal has longer arrival time at the downstream sensors due to the lower convection velocity, resulting in degradation of the prediction accuracy.

CONCLUSIONS

A machine-learning-based method for source prediction in turbulent channel was presented. This method predicted the source location and strength only using downstream sensor signals, without requiring flow field data. The results showed that the prediction accuracy depends on the source location. Sources located near the channel center were predicted accurately, while near-wall sources exhibited uncertainty in the streamwise location due to enhanced diffusion of the scalar field. The present method provides fast predictions and is suitable for real-time applications such as source detection in semiconductor fabs.

ACKNOWLEDGEMENTS

This work is supported by Samsung Advanced Institute of Technology, Korea.

REFERENCES

Gualtieri, L., Stutzmann, E., Juretzek, C., Hadziioannou, C., and Ardhuin, F., 2019, "Global Scale Analysis and Modelling of Primary Microseisms", *Geophysical Journal International*, Vol. 218, No. 1, pp. 560-572.

Massman, W. J., 1998, "A Review of the Molecular Diffusivities of H2O, CO2, CH4, CO, O3, SO2, NH3, N2O, NO, and NO2 in Air, O2 and N2 Near STP", *Atmospheric Environment*, Vol. 32, No. 6, pp. 1111-1127.

Wang, Q., Hasegawa, Y., and Zaki, T. A., 2019, "Spatial Reconstruction of Steady Scalar Sources from Remote Measurements in Turbulent Flow", *Journal of Fluid Mechanics*, Vol. 870, pp. 316-352.

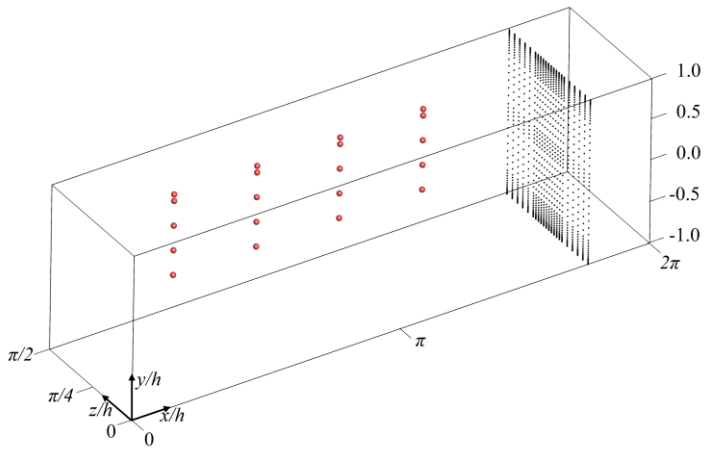

Figure 1. Red circles represent the actual source locations, while black ones are the positions of 1474 sensors for measuring scalar signals. The sources are located on a z-plane ($z = \pi/4$), whereas the sensors are arranged on an x-plane ($x = 5.52h$). The source locations are distributed uniformly in the streamwise direction and finer near the wall in the wall-normal direction. The sensors are non-uniformly distributed: more near the wall in the wall-normal direction than at the channel center, and more at the source z location than other spanwise location.

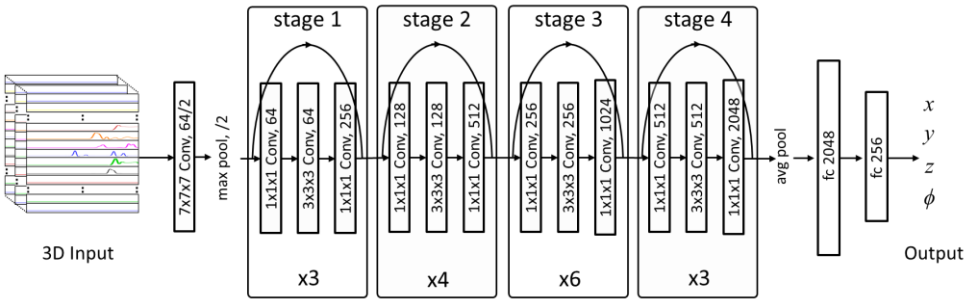

Figure 2. Architecture of the proposed 3D ResNet-50 for sensor-data–based source prediction. The input tensor passes through two stem convolutions, followed by four residual blocks. Spatial downsampling is performed via max pooling between and after the stem convolutions. Global average pooling produces a feature vector, which is then flattened and fed to fully connected layers to predict the source coordinates and strength.

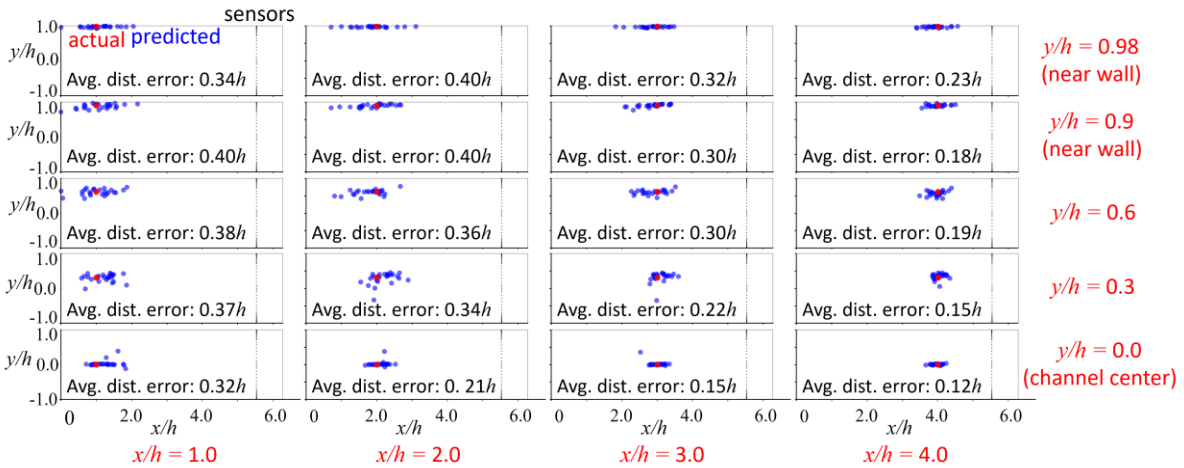

Figure 3. Prediction results for 20 different source locations at x/h = 1.0, 2.0, 3.0, and 4.0 and y/h = 0, 0.3, 0.6, 0.9, and 0.98. Each plot shows the predicted source locations (blue dots) and the actual source location (red dot). Average distance errors are shown in this figure.